

## Research Article

# The Luminescent Properties and Atomic Structures of As-Grown and Annealed Nanostructured Silicon Rich Oxide Thin Films

**N. D. Espinosa-Torres, J. A. D. Hernández-de-la-Luz, J. Martínez-Juárez,  
J. F. J. Flores-Gracia, and J. A. Luna-López**

*CIDS-ICUAP Benemérita Universidad Autónoma de Puebla, C.U., Edif. 103 C-D, Col. San Manuel, 72570 Puebla, PUE, Mexico*

Correspondence should be addressed to N. D. Espinosa-Torres; [siox130@gmail.com](mailto:siox130@gmail.com)

Received 5 June 2016; Revised 10 September 2016; Accepted 3 October 2016

Academic Editor: Wenrui Zhang

Copyright © 2016 N. D. Espinosa-Torres et al. This is an open access article distributed under the Creative Commons Attribution License, which permits unrestricted use, distribution, and reproduction in any medium, provided the original work is properly cited.

Not long ago, we developed a theoretical model to describe a set of chemical reactions that can potentially occur during the process of obtaining Silicon Rich Oxide (SRO) films, an off stoichiometry material, notwithstanding the technique used to grow such films. In order to elucidate the physical chemistry properties of such material, we suggested the chemical reactions that occur during the process of growing of SRO films in particular for the case of the Low Pressure Chemical Vapor Deposition (LPCVD) technique in the aforementioned model. The present paper represents a step further with respect to the previous (published) work, since it is dedicated to the calculation by Density Functional Theory (DFT) of the optical and electronic properties of the as-grown and annealed SRO structures theoretically predicted on the basis of the previous work. In this work, we suggest and evaluate either some types of molecules or resulting nanostructures and we predict theoretically, by applying the DFT, the contribution that they may have to the phenomenon of luminescence (PL), which is experimentally measured in SRO films. We evaluated the optical and electronic properties of both the as-grown and the annealed structures.

## 1. Introduction

SRO thin films have been studied lengthily and are very fascinating due to their optoelectronic properties, particularly those related with luminescence. In general, the luminescent properties can provide significant information regarding the crystalline structure of a material and, in the case of SRO thin films, their luminescence properties are considered of great importance since these films can be used to fabricate luminescent devices [1].

When SRO thin films are annealed, the oxides are degraded. For example, for  $\text{SiO}_2$  and  $\text{Si}_2\text{O}_3$  the believable annealing reactions were proposed by Espinosa-Torres [2], although the possibility that other oxides could be formed during the deposition process exists.

A well-known fact, as reported in scientific works, is that SRO films can be obtained, among other techniques, by using the LPCVD technique employing silane and nitrous oxide as precursory gases. The key effect of thermal treatment

consists in the development of structural transformations due to elimination of oxygen and hydrogen atoms, which leads as final result to the formation of small agglomerates of silicon atoms and defects due to the vacancies of oxygen atoms. It is worth noting that the as-grown SRO films could contain substoichiometric oxides and nanoparticles of silicon (Si-nps). Fourier Transform Infrared (FTIR) measurements evidenced that thermal annealing results in a phase separation and then Si-nps embedded in stoichiometric oxide matrix are produced [3]. However, to date there is no clear explanation on the increase of photoluminescence after the heat treatment in films SiOx obtained experimentally. The PL has been linked to the formation of silicon nanocrystals or to defects formed in the matrix and interface SiOx-Si-ncs. As a consequence, this is a clear motivation for this simulation in order to try to discern which of these phenomena contributes to the PL emission. Therefore these theoretical calculations are intended to model the behavior of the structures proposed to approximate their FTIR spectra, PL, and UV-Vis to the

TABLE 1: Comparison of experimental results versus theoretical calculations. Energy of the optical bang gap obtained experimentally by Tauc's method for SRO films with different Ro values and times of thermal treatment.

Ro	Band gap, (eV)			Structure	Calculated band gap, (eV)
	30 min	Annealed at 1100°C (experimental results) 60 min	180 min		
10	2.4 ± 0.04	2.4 ± 0.02	<b>2.43 ± 0.04</b>	Si <sub>11</sub> O <sub>11</sub> :H <sub>12</sub> (completely hydrogen saturated structure or as-grown structure)	5.766
20	3.57 ± 0.03	3.6 ± 0.06	<b>3.69 ± 0.03</b>	Si <sub>11</sub> O <sub>11</sub> (fully annealed structure)	<b>2.709</b>
30	3.73 ± 0.06	3.86 ± 0.04	<b>3.89 ± 0.04</b>	Si <sub>14</sub> O <sub>14</sub> :H <sub>12</sub>	5.221
				Si <sub>14</sub> O <sub>14</sub> :H <sub>10</sub>	4.656
				Si <sub>14</sub> O <sub>14</sub> :H <sub>8</sub>	4.611
				Si <sub>14</sub> O <sub>14</sub> :H <sub>6</sub>	4.495
				Si <sub>14</sub> O <sub>14</sub> :H <sub>4</sub>	4.404
				Si <sub>14</sub> O <sub>14</sub> (fully annealed structure)	<b>3.256</b>

spectra obtained experimentally in order to understand, which are the physical processes that allow us to explain the observed PL.

In this research, we employed the Density Functional Theory with a functional B3LYP and a basis set 6-31 G\* to calculate the optical and electronic properties of Si<sub>n</sub>O<sub>n</sub> and Si<sub>n</sub>O<sub>n</sub>:H<sub>x</sub> nanostructures with the aim of contributing to a better understanding of the luminescent phenomena observed in the SRO thin films. In a previous published work [4], we have already modeled different silicon nanoclusters, so in the present paper we only focus on the Si<sub>n</sub>O<sub>n</sub> oxide structures.

## 2. Results and Discussion

**2.1. Band Gap Calculations.** There are different factors that have an important influence on the optical properties of the SRO films. Factors such as the support substrate type, silicon excess, annealing temperatures, time of thermal treatment, and composition at deposition moment and subsequent transformations are very important factors which play an important role to determine the optical properties of the SRO films. Particularly, PL of samples deposited by LPCVD also depends on the partial pressure ratio between N<sub>2</sub>O and SiH<sub>4</sub> defined as Ro = [N<sub>2</sub>O/SiH<sub>4</sub>] and thermal annealing conditions [5].

In Table 1 we present our results for theoretically calculated values of band gaps for the structures Si<sub>11</sub>O<sub>11</sub>H<sub>12</sub>, Si<sub>11</sub>O<sub>11</sub>, Si<sub>14</sub>O<sub>14</sub>, and Si<sub>14</sub>O<sub>14</sub>H<sub>m</sub> ( $m = 12, 10, 8, 6,$  and  $4$ ). We consider that Si<sub>11</sub>O<sub>11</sub> and Si<sub>14</sub>O<sub>14</sub> refer to the fully annealed oxides, whereas Si<sub>11</sub>O<sub>11</sub>H<sub>12</sub> and Si<sub>14</sub>O<sub>14</sub>H<sub>12</sub> refer to the as-grown oxides. In Table 1, the experimental values of band gaps obtained in [5] for the SRO with different Ro and different times of annealing at 1200°C are presented. The experimental values were obtained by Tauc method proposed for amorphous materials. In general, for the annealing time of 180 min, the SRO films could be considered as fully annealed (dehydrogenated). As one can see, the calculated values for Si<sub>11</sub>O<sub>11</sub> and Si<sub>14</sub>O<sub>14</sub> lie in the interval of experimental values

for the annealed SRO. Moreover, the calculated value of band gap for Si<sub>14</sub>O<sub>14</sub> is greater than that for Si<sub>11</sub>O<sub>11</sub>. It is probable that in the annealed SRO with Ro ≥ 20 [5] (see Table 1) the number of Si or O atoms in the Si<sub>n</sub>O<sub>n</sub> structure is greater than 16.

**2.2. FTIR and PL Calculations.** The FTIR and PL spectra given in Figure 1 are the first results obtained of our numerical simulations for atomic structures of the type Si<sub>n</sub>O<sub>n</sub>:H<sub>m</sub>. In the right side of Figure 1, we display the calculated molecular structure, considered as-grown, for Si<sub>11</sub>O<sub>11</sub>:H<sub>12</sub> (a) and in (b) the new structure, that is, when it has been fully annealed: Si<sub>11</sub>O<sub>11</sub>. The most remarkable difference is observed in the correspondent FTIR (top of both figures). The as-grown structure displays vibrational frequencies due to Si-H bonds in a frequency of 2281.404 cm<sup>-1</sup> and the structure after annealing process does not exhibit any vibration around this frequency. Also, in Figure 1 we can observe that the structure as-grown (Si<sub>11</sub>O<sub>11</sub>:H<sub>12</sub>) emits energy in the violet region (Figure 1(a)), while the corresponding annealed structure, displayed on Figure 1(b), which corresponds with PL spectrum for Si<sub>11</sub>O<sub>11</sub>, is also able to emit light in visible region.

Also, in Figure 1 are displayed the corresponding structures for Si<sub>11</sub>O<sub>11</sub>:H<sub>12</sub> and Si<sub>11</sub>O<sub>11</sub>. For the structure Si<sub>11</sub>O<sub>11</sub>:H<sub>12</sub> we have incorporated the electrostatic potential map (an electrophilic indicator) for an isovalue of -83.68 KJ/mol, and we have labeled the silicon, oxygen, and hydrogen atoms. This gives the electrostatic potential at locations on a particular surface, most commonly a surface of electron density corresponding to overall molecular size [6], whereas, for the Si<sub>11</sub>O<sub>11</sub> structure, we have included the Local Ionization Potential Map (LIPM) for an isovalue of 20 (without units or dimensionless). LIPM reflects the relative straightforwardness of electron removal ("ionization") at any location around a molecule. The numbers near the different atoms in the structure Si<sub>11</sub>O<sub>11</sub> are the calculated Mulliken charges.

FTIR vibrations modes and their corresponding frequency of vibrations in the as-deposited and after annealed

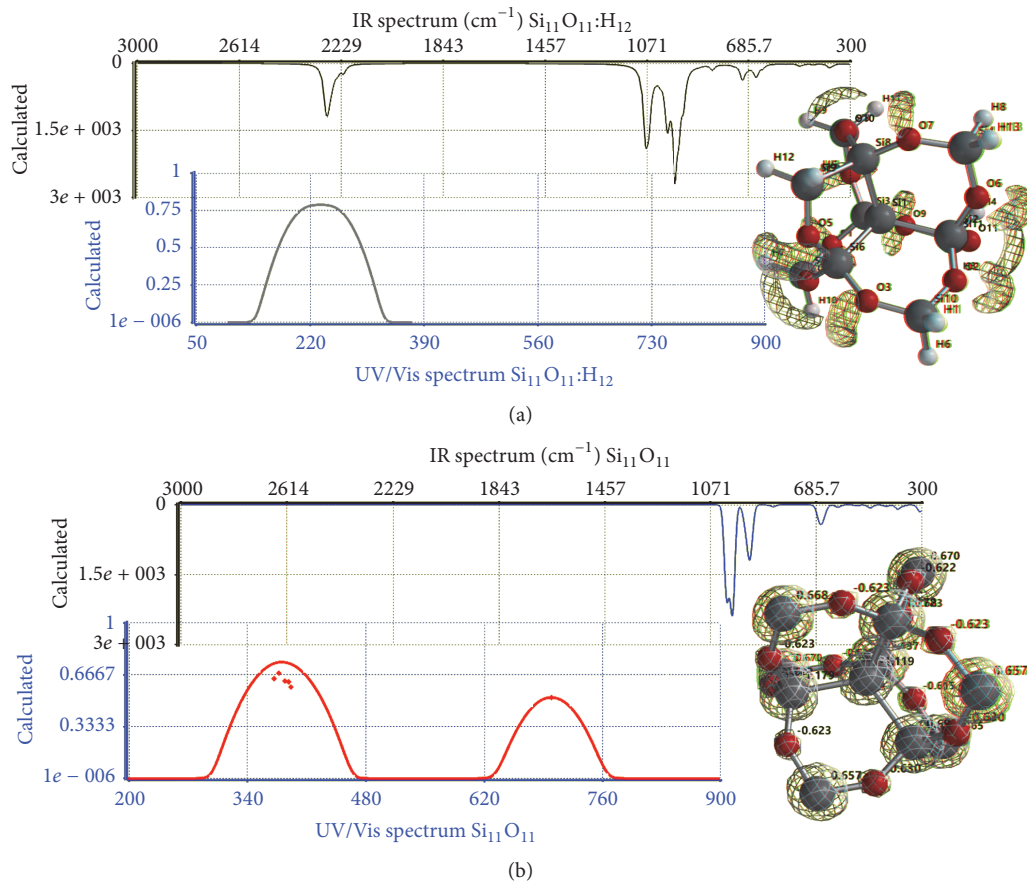


FIGURE 1: (a) Molecular structure with eleven silicon atoms  $\text{Si}_{11}\text{O}_{11}:\text{H}_{12}$  (as-grown), UV/Vis spectrum with only one luminescence peak in UV region and IR spectrum with a peak due to Si-H bond; (b) fully annealed  $\text{Si}_{11}\text{O}_{11}$  molecular nanostructure, UV-Vis spectrum displaying luminescence in two regions (UV and visible) and IR spectrum without peak owing to Si-H bond.

SRO films, considering silica and SRO films with different values of  $R_o$ , are consigned in literature [2]. The values commonly found are Si-O rocking  $458\text{--}450\text{ cm}^{-1}$ , Si-O bending  $815\text{--}805\text{ cm}^{-1}$ , Si-O stretching on phase  $1061\text{--}1082\text{ cm}^{-1}$ , and Si-O stretching out of phase  $1160\text{--}1185\text{ cm}^{-1}$ .

The three most intense peaks in the calculated FTIR spectra of as-grown structure correspond with frequencies of  $962.355$ ,  $995.002$ , and  $1067.44\text{ cm}^{-1}$ . It was found that the total number of calculated vibrations for as-grown structure was 96 different modes. The last one value of frequency calculated ( $1067.44\text{ cm}^{-1}$ ) fits well with experimental data previously reported for Si-O stretching on phase, whereas for the annealed structure the three most intense peaks calculated were  $930.909$ ,  $990.752$ , and  $1012.774\text{ cm}^{-1}$  and there are only 60 frequencies of vibration (there are no longer Si-H bonds). These results obtained suggest that SRO films experimentally annealed were not completely passivated.

The calculated proposal includes structures type  $\text{Si}_{11}\text{O}_{11}$ , which contain twelve Si-Si bonds. The annealed structure  $\text{Si}_{11}\text{O}_{11}$  gives us a frequency of vibration at  $669.029\text{ cm}^{-1}$  and we confirm that it is due to Si-Si bonds. Again, these results have a good correlation with experimental results earlier reported for  $R_o = 30$  [7, 8]. With respect to as-grown and

thermally treated PL calculated spectra, we predict luminescence in ultraviolet region in  $251.34\text{ nm}$  in only one band for the film originally deposited. When the nanostructure is fully passivated, this band moves or shifts to  $377.58\text{ nm}$  (yet in ultraviolet) and a second band of emission centered at  $699.24\text{ nm}$  appears, giving a red emission.

Emission in red region has been evidenced experimentally for SRO films with  $R_o = 10, 20$ , and  $30$ , but the movement of the band into ultraviolet region has not been noticed or it has not yet been reported, probably due to the interest focused on only in emission in visible region.

Figure 2 displays the calculated FTIR spectra for different silicon oxide clusters size for structures fully annealed (dehydrogenated)  $\text{Si}_n\text{O}_n$  for  $n = 5, 11, 14, 16, 17$ , and  $19$ . We have constructed the Gaussian type curves with  $\text{FWHM} = 20\text{ nm}$  and selected the scale from  $300$  to  $1500\text{ cm}^{-1}$  (there are not any data calculated beyond this interval). For the intensities we choose a scale of  $0\text{--}4000$  in arbitrary units for all the cases presented in Figure 2. Only in the spectrum which corresponds with  $n = 16$  we predicted the Si-O rocking type vibrations in interval from  $417$  to  $429\text{ cm}^{-1}$  and it has a quite small intensity. A probable explanation for this fact is that Si-O rocking type vibration observed experimentally could

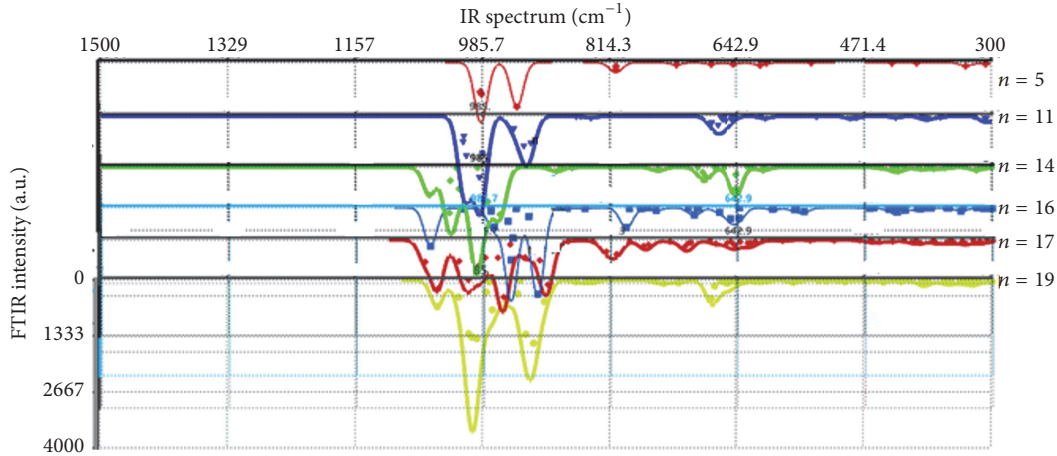


FIGURE 2: FTIR spectra calculated for  $\text{Si}_n\text{O}_n$  (fully annealed structures), varying the number of silicon atoms for  $n = 5, 11, 14, 16, 17,$  and  $19$ .

be due to other kinds of oxides existing in SRO thin films, like  $\text{SiO}_2$  and  $\text{Si}_2\text{O}_3$  [9].

The intensity of the frequencies of vibration for bonds Si-O is increased accordingly as the number of silicon atoms is increased in the agglomerates studied. The vibrations calculated, during the numerical simulations, for bending type Si-O bond were predicted in the interval from  $751$  to  $840\text{ cm}^{-1}$  as follows:  $n = 5$  ( $806$ ),  $n = 11$  ( $840$ ),  $n = 14$  ( $751$ ),  $n = 16$  ( $794$ ),  $n = 17$  ( $821$ ), and  $n = 19$  ( $833$ ). Some of these vibrations have a quite small intensity and they are not visible to the naked eye.

For the second stage of this study, we choose a bigger structure ( $\text{Si}_{14}\text{O}_{14}$ ) but maintaining the Si/O ratio. Figure 2 corresponds with as-grown case. The analysis and discussion are similar to the structure shown in the first stage of this study, and as relevant results we found that there are only small variations in the values calculated; for example, the frequency vibration due to Si-H bond appears in the frequency interval from  $2262.084$  to  $2307.217\text{ cm}^{-1}$ , being the most intense at  $2265.384\text{ cm}^{-1}$ . Of course, in the cited interval there are twelve calculated vibrations due to Si-H bond. Only in the structure which corresponds with fully annealed condition the vibration due to Si-H vanishes completely.

In Figures 3–8 we present results of an evolution in the structure assuming the constant loss of pairs of hydrogen atoms. The points drawn outside of the curves in FTIR and PL spectra in Figures 3–8 correspond with the vibrational frequencies calculated and the points displayed in PL spectra are the wavelength of calculated emission states. Then the curves correspond with the predicted observable spectra. The points calculated for the frequencies of vibration in FTIR spectra and the wavelengths of emission in PL spectra, being in close proximity, add constructively. As a result of the foregoing, an increase in the intensity of the spectra will be observed. Therefore the solid line in the resulting spectra observed will not always cross the calculated points. The width of the peaks in the spectra of vibration and width of the luminescent bands will depend on the thickness of the SRO films.

Numerical data are consigned in Table 2. We predict again the shift of the ultraviolet band. For structures type  $\text{Si}_{14}\text{O}_{14}$  we confirm that there is only one band which resembles two bands overlapped. The results predict emission in a wide range from violet to orange color. Experimentally, the luminescence in this range has been reported due to cathode luminescence in SRO films (see Figure 8 of [10]) for as-grown and annealed films, mainly for  $\text{Ro} = 20$  and  $30$ , when an energy excitation of  $5\text{ keV}$  and  $0.3\text{ mA}$  current was used [9]. Additionally, the interested audience in experimental emission of as-grown SRO films with  $\text{Ro} = 30$  is motivated to review [11].

Data in Table 2, for wavelength with the highest intensity of emission (nm) in UV-Vis spectrum, fits exactly with the next quadratic equation:

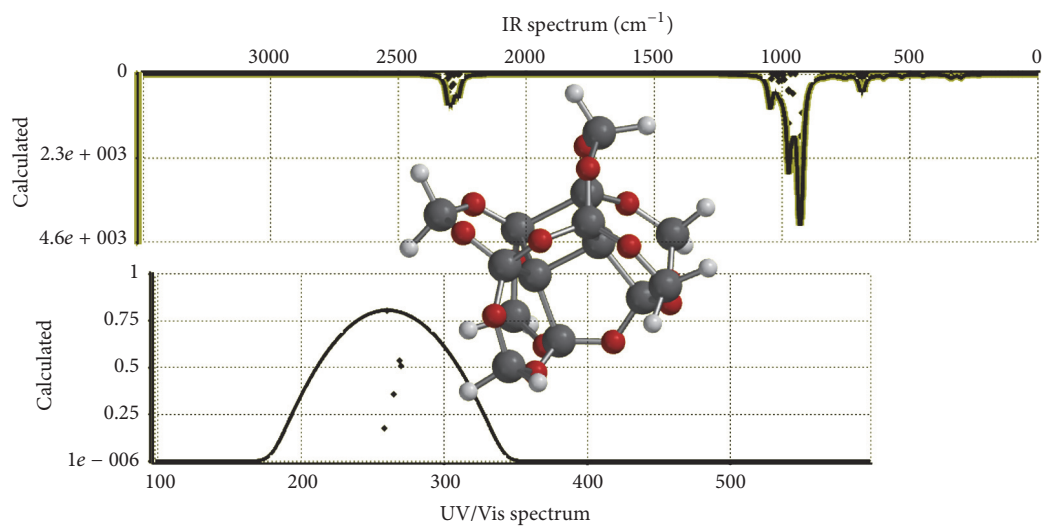
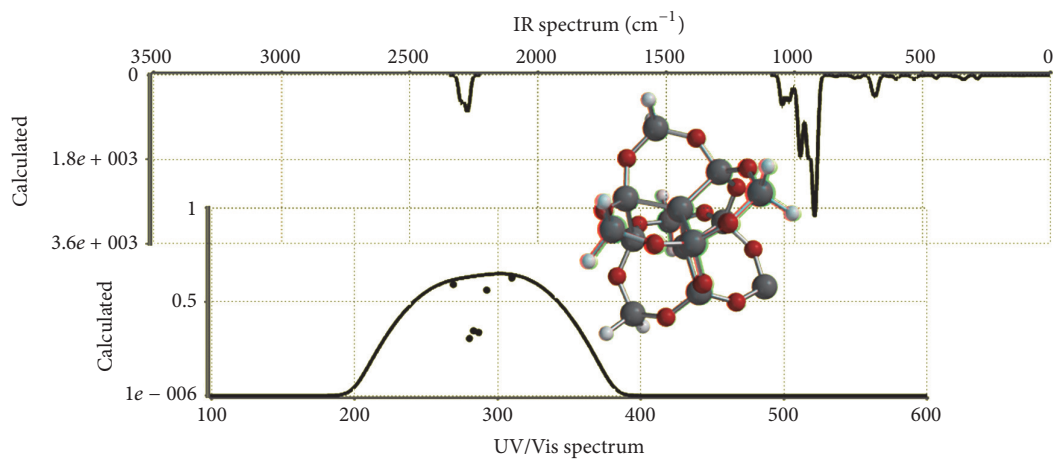
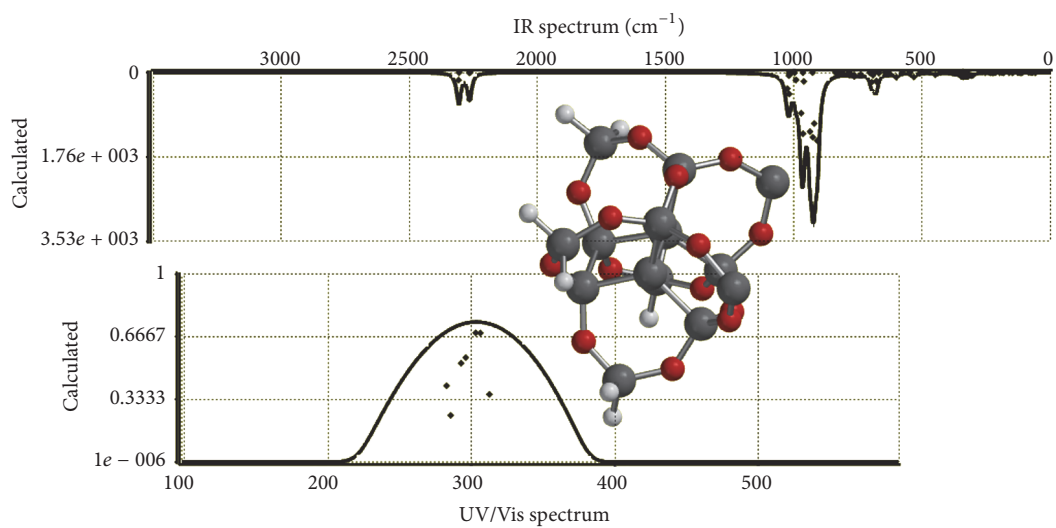
$$\lambda = 4.9542n^2 - 51.442n + 444.4. \quad (1)$$

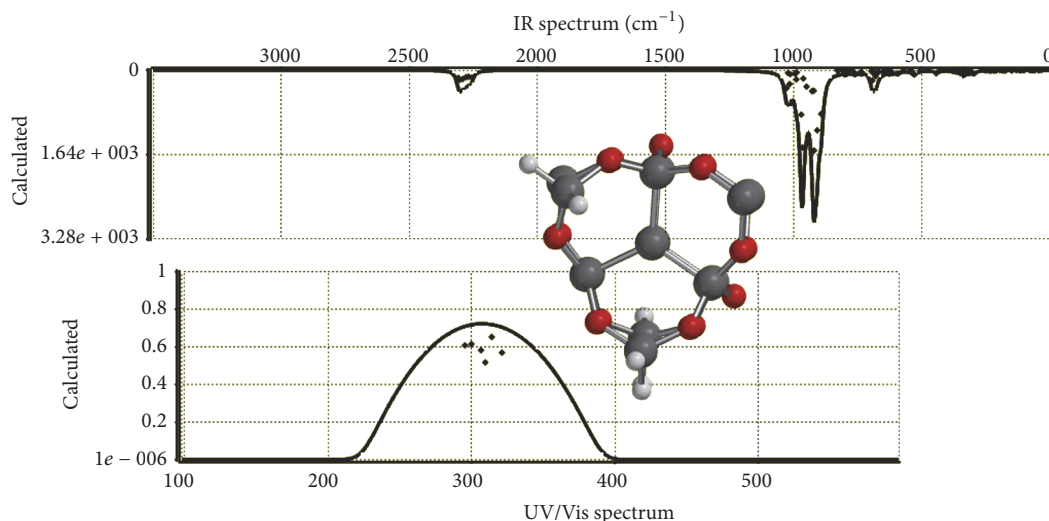
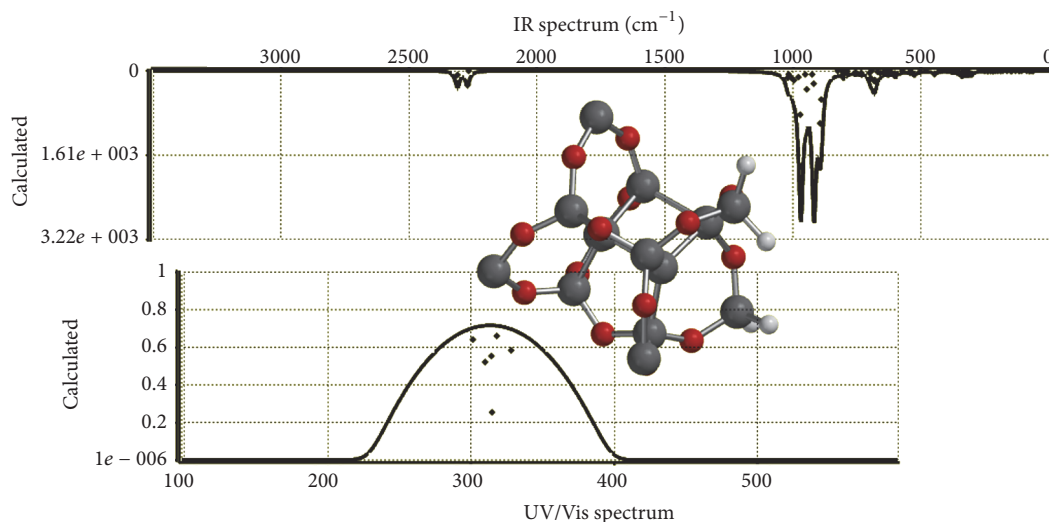
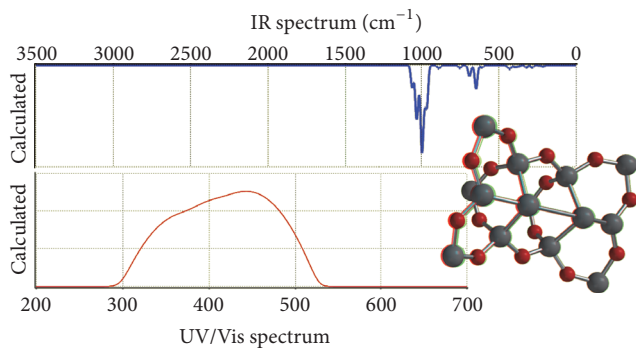
With  $R^2 = 1$ , in this equation  $\lambda$  is the highest intensity of emission (nm) and  $n$  is the number of hydrogen atoms in the structure.

Unfortunately, it is not easy to give an acceptable explanation of this finding in this moment, because there are necessary additional studies of the kinetic of set of reactions, and experimentally it is not possible to isolate only one reaction during the deposition process.

Regarding Figure 8,  $\text{Si}_{14}\text{O}_{14}$  displays a wide emission range, which looks like two bands overlapped. Theoretically it is possible to model the thickness of SRO samples varying the FWHH and in this way we can obtain a separated two-band spectrum. In our simulations, we apply the FWHH value which corresponds to experimental samples typically found in the literature in which usually PL spectrum with a single band is reported. Then, our calculations predict the possibility of new mechanisms for emission in SRO thin films with an “extreme dwarf thickness.”

The experimental FTIR absorption spectra of as-grown and thermally treated SRO films with different silicon excess that are shown in Figure 9 were adapted from Espinosa-Torres [2]. The original interval for experimental data displayed

FIGURE 3: Case  $\text{Si}_{14}\text{O}_{14}:\text{H}_{12}$ .FIGURE 4: Case  $\text{Si}_{14}\text{O}_{14}:\text{H}_{10}$ .FIGURE 5: Case  $\text{Si}_{14}\text{O}_{14}:\text{H}_8$ .

FIGURE 6: Case  $\text{Si}_{14}\text{O}_{14}\cdot\text{H}_6$ .FIGURE 7: Case  $\text{Si}_{14}\text{O}_{14}\cdot\text{H}_4$ .FIGURE 8: Case  $\text{Si}_{14}\text{O}_{14}$ .

in Figure 9 ranges from 500 to 2000  $\text{cm}^{-1}$  and the plot is extended up to 2125  $\text{cm}^{-1}$ , but there is not any data beyond,

which means that no experimental data were reported in the cited reference for the Si-H bond. The spectrum of the thermal  $\text{SiO}_2$  structure is also shown as a reference in curve 1. These spectra show the absorption peaks associated with stretching (1084  $\text{cm}^{-1}$ ), bending (812  $\text{cm}^{-1}$ ), and rocking (458  $\text{cm}^{-1}$ ) vibration modes of the Si-O-Si bonds in  $\text{SiO}_2$  [10, 12, 13]. The position of the stretching absorption peak changes with the Ro value and with thermal treatments. In Figure 9, the abbreviation TT is employed to describe thermal treatment and AG refers to as-grown.

Despite the structural shape of the molecular structures shown in Figures 3–8, the structures are not quite different between them, except for the number of hydrogen atoms introduced. Intentionally the structures were rotated to give to the reader the best perspective of the atomic arrangement.

In this report, we have theoretically predicted a shift of the Si-O stretching on phase vibration peak toward higher

TABLE 2: Calculated optical properties for structures type  $\text{Si}_{14}\text{O}_{14}:\text{H}_n$ .

Reference	Structure	Wavelength with the highest intensity emission (nm) in UV-Vis spectrum	Frequency peak with the highest intensity $\text{cm}^{-1}$ (due to Si-O bonds) in FTIR spectrum	Frequency due to Si-H bonds $\text{cm}^{-1}$ (only peaks with the highest intensities in FTIR spectrum are shown)
Figure 3	$\text{Si}_{14}\text{O}_{14}:\text{H}_{12}$	268.7	934	2306
Figure 4	$\text{Si}_{14}\text{O}_{14}:\text{H}_{10}$	292.5	925	2300
Figure 5	$\text{Si}_{14}\text{O}_{14}:\text{H}_8$	303–306.2	926	2264 and 2306
Figure 6	$\text{Si}_{14}\text{O}_{14}:\text{H}_6$	314.1	922	2302
Figure 7	$\text{Si}_{14}\text{O}_{14}:\text{H}_4$	317.9	925	2271 and 2309
Figure 8	$\text{Si}_{14}\text{O}_{14}$	444.4	996	It does not exist

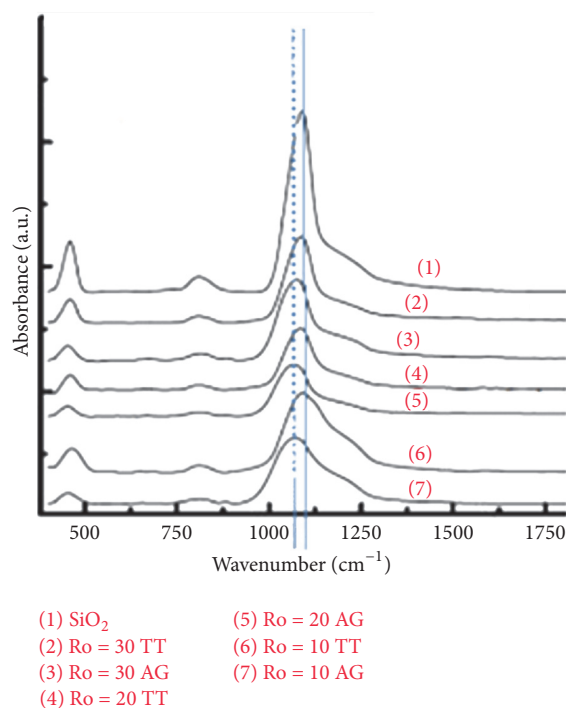


FIGURE 9: Experimental results for SRO films. The mismatched values for the experimental and theoretical peak positions are mainly attributed to the fact that reported experimental data are a mixture of silicon oxides, known as SRO, and in this work we only evaluated a single type of silicon oxide, namely, the ( $\text{Si}_n\text{O}_n$ ) structure. Adapted from Luna-López et al. [3].

energies accordingly as the number of hydrogen atoms is reduced (Table 2). This shift is experimentally confirmed by the experimental spectra reported in Figure 9, since the thermal annealing treatment of the SRO films produces a shift of the peak corresponding to the Si-O stretching on phase vibration toward higher energies, regardless of the Ro value employed.

The Si-O stretching on phase vibration was predicted to be positioned in the range from 934 to 996  $\text{cm}^{-1}$ , as the number of H atoms reduces from 12 to zero in  $\text{Si}_{14}\text{O}_{14}:\text{H}_x$  structures. However, Luna-López et al. [3] find this peak shifted to 1061–1088  $\text{cm}^{-1}$  in the experimental spectra of SRO

films deposited with different values of Ro = 10, 20, and 30 (Table 1 of [3]).

### 3. Conclusions

In this work, we have applied the model known as the Global Reaction Model in order to predict the theoretical luminescent behavior of the as-grown and annealed nanostructured Silicon Rich Oxide films where we have focused on the presence of hydrogen atoms as the key factor. We evaluate the PL spectrum of the as-grown SRO samples and also after the annealing procedure in which such samples are submitted and we have given evidence of the luminescent emission in the visible region of electromagnetic spectra, when the samples are fully dehydrogenated. Also, we calculated the theoretical FTIR spectra for as-grown and for partially and fully annealed structures. We have made comparisons of the results, obtained in this research, with those obtained experimentally, which have been reported in literature and we have found evidence of a good agreement between them. After making a comparison of the experimental and calculated band gaps, PL, and FTIR spectra, it conducts us to conclude that agglomerates type Si-O with a number of silicon atoms of eleven and fourteen would be present in SRO films deposited for  $10 < \text{Ro} < 20$ . Finally, we can conclude that SRO films as-deposited frequently are not fully saturated.

### Disclosure

The current affiliation for N. D. Espinosa-Torres, Postdoctoral Fellow, is Instituto de Energías Renovables, UNAM Campus Temixco, Privada Xochicalco s/n, 62580 Temixco, MOR, Mexico.

### Competing Interests

The authors declare that there is no conflict of interests regarding the publication of this manuscript.

### Acknowledgments

This work was supported by project VIEP-HEDJ-EXC16-I and Cuerpo Académico “Semiconductores Nanoestructurados y Orgánicos,” BUAP-CA-275.

## References

- [1] P. Mutti, G. Ghislotti, S. Bertoni et al., "Room-temperature visible luminescence from silicon nanocrystals in silicon implanted SiO<sub>2</sub> layers," *Applied Physics Letters*, vol. 6, no. 7, pp. 851–853, 1995.
- [2] N. D. Espinosa-Torres, *Theoretical study of the luminescent phenomena in silicon rich oxide [Ph.D. thesis]*, Centro de Investigación en Dispositivos Semiconductores, BUAP, 2015.
- [3] J. A. Luna-López, J. Carrillo-López, M. Aceves-Mijares, A. Morales-Sánchez, and C. Falcony, "FTIR and photoluminescence of annealed silicon rich oxide films," *Superficies y Vacío*, vol. 22, no. 1, pp. 11–14, 2009, marzo de 2009 ©Sociedad Mexicana de Ciencia y Tecnología de Superficies y Materiales.
- [4] N. D. E. Torres, J. F. J. F. Gracia, and J. A. L. López, "Ab initio molecular orbital calculation for optical and electronic properties evaluation of small and medium size silicon nanoclusters found in silicon rich oxide films," *Journal of Modern Physics*, vol. 4, pp. 1–26, 2013.
- [5] J. A. Luna-López, M. Aceves-Mijares, J. Carrillo-López, A. Morales-Sánchez, F. Flores-Gracia, and D. E. Vázquez Valerdi, "UV-Vis photodetector with silicon nanoparticles," in *Photodetectors*, S. Gateva, Ed., InTech, 2012.
- [6] Spartan Tutorial, User's Guide Hehre, J. Warren, and W. S. Ohlinger, *Spartan'14 Tutorial and User's Guide*, Wavefunction, Inc., Irvine, Calif, USA, 2013.
- [7] T. Morioka, S. Kimura, N. Tsuda, C. Kaito, Y. Saito, and C. Koike, "Study of the structure of silica film by infrared spectroscopy and electron diffraction analyses," *Monthly Notices of the Royal Astronomical Society*, vol. 299, pp. 78–82, 1998.
- [8] T. Inokuma, Y. Kurata, and S. Hasewaga, "Cathodoluminescence properties of silicon nanocrystallites embedded in silicon oxide thin films," *Journal of Luminescence*, vol. 80, no. 1–4, pp. 247–251, 1998.
- [9] R. López-Estopier, M. Aceves-Mijares, and C. Falcony, "Cathodo- and photo- luminescence of silicon rich oxide films obtained by LPCVD," in *Cathodoluminescence*, N. Yamamoto, Ed., InTech, 2012, <http://www.itspozarica.edu.mx/carreras/documentos/electronica/InTech-Cathodo.pdf>.
- [10] M. Aceves, D. Berman, J. Carranza, L. Berriel, and C. Domínguez, "UV DETECTORS: silicon-rich silicon oxide films boost UV sensitivity," *Laser Focus World*, vol. 41, no. 9, pp. 103–105, 2005.
- [11] M. Aceves-Mijares, N. D. Espinosa-Torres, F. Flores-Gracia et al., "Composition and emission characterization and computational simulation of silicon rich oxide films obtained by LPCVD," *Surface and Interface Analysis*, vol. 46, no. 4, pp. 216–223, 2014.
- [12] F. Ay and A. Aydinly, "Comparative investigation of hydrogen bonding in silicon based PECVD grown dielectrics for optical waveguides," *Optical Materials*, vol. 26, no. 1, pp. 33–46, 2004.
- [13] P. G. Pai, S. S. Chao, Y. Takagi, and G. Lucovsky, "Infrared spectroscopic study of siox films produced by plasma enhanced chemical vapor-deposition," *Journal of Vacuum Science & Technology A: Vacuum, Surfaces, and Films*, vol. 4, no. 3, pp. 689–694, 1986.



**Hindawi**

Submit your manuscripts at  
<http://www.hindawi.com>

